Proc. Natl. Acad. Sci. USA
Vol. 95, pp. 11101–11106, September 1998
Biochemistry

Effects of transition metals on nitric oxide synthase catalysis

JASON M. PERRY* AND MICHAEL A. MARLETTA*†‡

*Interdepartmental Program in Medicinal Chemistry, College of Pharmacy, †Department of Biological Chemistry, School of Medicine, and ‡The Howard Hughes Medical Institute, University of Michigan, Ann Arbor, MI 48109-1065

Communicated by Vincent Massey, University of Michigan Medical School, Ann Arbor, MI, July 9, 1998 (received for review April 21, 1998)

ABSTRACT **The biosynthesis of nitric oxide (NO) by the enzyme NO synthase (NOS) proceeds by the hydroxylation of L-arginine to form N^G-hydroxy-L-arginine followed by the conversion of N^G-hydroxy-L-arginine to L-citrulline and NO. The previously identified requirements of this relatively complicated reaction include several protein-bound cofactors: cytochrome P450-type heme, flavin mononucleotide (FMN), flavin adenine dinucleotide (FAD), and tetrahydrobiopterin (H_4B). In addition to L-arginine, NOS also requires the substrates NADPH and molecular oxygen. The role of H_4B in NOS catalysis has long been a subject of debate and uncertainty fueled, in part, by the failure to detect any dependence of the NOS reaction on nonheme iron, a cofactor integral to catalysis in every other H_4B-dependent enzyme. Here we report the ability of NOS to bind transition metals stoichiometrically, and demonstrate that the rate of catalysis is enhanced by nonheme iron. We also show that other divalent transition metals, including Cu, Zn, Co, and Ni, inhibit NOS catalysis. Also, the addition of Cu^{2+} to NOS inhibits heme reduction, whereas the addition of Fe^{2+} does not. Overall, the results appear to connect NOS to the known H_4B/nonheme iron-dependent hydroxylases, and suggest a similar, if not identical, step in the NOS reaction mechanism.**

Nitric oxide (NO) synthase (NOS; EC 1.14.13.39) catalyzes the oxidative conversion of L-arginine to NO and citrulline through an NADPH-dependent reaction. NO has been shown to be both a signal transduction agent that stimulates the soluble isoform of guanylate cyclase and a component of the host response to infection; further, it is a putative participant in processes such as neuronal development and apoptosis (1). There are two classes of NOS isoforms: the constitutive isoforms, which are activated by the binding of a Ca^{2+}/calmodulin complex and were initially isolated from the cerebellum and endothelial smooth muscle tissue, and the cytokine-induced isoforms, which are regulated at transcription and copurify with calmodulin as a tightly bound subunit (2). For both classes, a homodimeric quaternary structure is requisite for catalytic activity, and each monomer subunit contains one equivalent each of FAD, FMN, (6*R*)-5,6,7,8-tetrahydro-L-biopterin (H_4B), and protoporphyrin IX heme (2). Electronically and magnetically the NOS heme resembles that of cytochrome P450 (P450) with a ferrous-CO complex λ_{max} at ≈445 nm (3) and, as expected, was found to be ligated by a protein-donated cysteine thiolate (4, 5). NOS also displays a high-spin shift of the heme iron in the presence of substrate. As with $P450_{BM3}$, the flavoprotein reductase and the cytochrome are contained within a single polypeptide; hence, catalysis does not rely on an interaction with another protein to supply NADPH-derived reducing equivalents to the active site, as is the case for almost all other known P450s.

The NOS reaction has been divided into two major steps after the discovery of the intermediate N^G-hydroxy-L-arginine (NHA) (6, 7). Recent results from our laboratory have implicated the NOS heme in the second partial reaction, the conversion of NHA to citrulline (by substituting the reduced oxygen species hydrogen peroxide for molecular oxygen and NADPH); however, hydrogen peroxide gave no reaction with L-arginine as the substrate (8, 9). In fact, there has never been any direct experimental evidence to support the hypothesis that the initial hydroxylation of L-arginine proceeds by the classical mixed-function oxidase P450 mechanism that invokes the formation of a high valent heme iron species as a result of O—O bond scission in a protic environment. Further, the recently solved crystal structure of the NOS oxygenase (heme) domain reveals that the distal pocket of the NOS heme is hydrophobic, an environment that favors a peroxide-mediated reaction such as that believed to occur in the conversion of NHA to NO and citrulline (5).

NOS is distinguished from all other known P450s by the requirement for H_4B. A direct role for H_4B in NOS catalysis has yet to be shown, but several proposals for its function have been advanced including: (*i*) binding as an allosteric effector, (*ii*) acting as a modulator of the potential inhibitory action of NO, and (*iii*) participation in the reaction as a redox-active cofactor in a manner analogous to all other H_4B-dependent enzymes, namely, in the hydroxylation of substrate—which in this case would be the conversion of L-arginine to NHA (10–12). The third possibility has received the least attention, in part, because the known requirement for nonheme iron by all of the H_4B-dependent hydroxylases has not been demonstrated for NOS. Herein we show that NOS can in fact bind transition metals and that reaction rate is enhanced by nonheme iron and inhibited by other divalent metals, which has led to the proposal that NOS could contain a nonheme iron/H_4B active site.

MATERIALS AND METHODS

Materials. 2′,5′-ADP-Sepharose, calmodulin-Sepharose 4B, disposable G-25M desalting columns (PD-10), and the HiLoad 26/60 Superdex-200 gel filtration column were obtained from Pharmacia. H_4B was purchased from B. Schircks Laboratories (Jona, Switzerland); 10 mM stock vials of this reagent were prepared in 50 mM Hepes buffer (pH 7.4) containing 100 mM DTT. L-[^{14}C]Arginine was from Amersham. *Escherichia coli* DH5α competent cells, T4 DNA ligase, and isopropyl β-D-thiogalactopyranoside (IPTG), were from GIBCO/BRL. All necessary restriction enzymes, ampicillin, and the Expand High Fidelity PCR kit were purchased from Boehringer Mannheim. The original cDNA clone for rat neuronal NOS contained in the vector Bluescript (SK$^-$) was a gift from Solomon H. Snyder (Johns Hopkins University, Baltimore), whereas the expression plasmid used, pCWori, was generously provided by Michael R. Waterman (Vanderbilt University, Nashville, TN). The standard solution used to calibrate atomic absorption measurements was from Alfa ÆSAR, and the Chelex 100 resin used to deplete adventitious metal ions from buffers and reagents was from

The publication costs of this article were defrayed in part by page charge payment. This article must therefore be hereby marked "*advertisement*" in accordance with 18 U.S.C. §1734 solely to indicate this fact.

Abbreviations: NOS, NO synthase; nNOS, neuronal NOS; iNOS, inducible NOS; NHA, N^G-hydroxy-L-arginine; H_4B, (6*R*)-5,6,7,8-tetrahydro-L-biopterin; P450, cytochrome P450; ICP, inductively coupled plasma atomic emission spectroscopy; PAH, phenylalanine hydroxylase.

Bio-Rad. All materials and reagents not described above were obtained from Sigma.

Cloning, Expression, and Purification. Techniques used to generate wild-type neuronal NOS (nNOS) and the nNOS C415A mutant were as reported elsewhere (13). The nNOS H652A mutant was generated by the PCR; the external primers were: 5′-GACCCTGAGCTCTTTCAGATCCCCCCAGAG-3′ and 5′-CCAGCTTCGGTCATTGCTAATGAGGGA-3′; the mutagenic primers were 5′-ATCGTTGACCAC*G*C̲CTCTGCCACG-GAGTCC-3′ and 5′-CGTGGCAGAG*G*C̲GTGGTCAACGAT-GGTCAC-3′. The fidelity of the PCR reactions was confirmed by DNA sequencing at the University of Michigan Biomedical Core Facility. Expression and purification conditions for nNOS H652A were identical to those used for wild-type nNOS (13). The oligomeric state of nNOS H652A was assessed by comparison of the gel filtration elution profile with that from various preparations of NOS of known oligomeric state (wild-type, dimer; C415A, heme ligand mutant, monomer). Expression methods for inducible NOS (iNOS) are analogous to those previously reported by Fossetta *et al*. (14), and purification was achieved by ADP-affinity chromatography using conditions as described (12) followed by size exclusion chromatography by using a HiLoad 26/60 Superdex-200 gel filtration column (buffer conditions: 100 mM Hepes/400 mM NaCl/10% vol/vol glycerol). H_4B (to 25 μM) was added to the sample before loading. The purity of all NOS proteins used in this study was >95%, as judged by SDS/PAGE analysis. Protein was quantified spectrophotometrically according to the method of Bradford (15).

Reconstitution of NOS with Iron. Reconstitution of NOS with nonheme iron was achieved by the incubation of ≈5 μM NOS in the presence of 5 mM L-arginine, 0.5 mM H_4B, 5 mM DTT, and 100 μM $FeCl_2$ in 50 mM Hepes (pH 7.4) at 0°C (on ice) for 5 min. Excess iron was subsequently removed by gel filtration, as described below.

Preparation of Samples for Metal Quantitation. Samples for inductively coupled plasma atomic emission spectroscopy (ICP) and graphite furnace atomic absorption spectroscopy, were prepared by using metal-free technique. Briefly, samples were desalted on a PD-10 G-25 column pre-equilibrated with metal depleted buffer, which was prepared by slowly passing 50 mM Hepes (pH 7.4) over a Chelex-100 column; when nonheme iron was reconstituted, the desalting procedure was carried out in the presence of 5 mM L-arginine and repeated twice on each sample to ensure the removal of any nonspecifically bound metal ions. ICP of nNOS samples (Leeman Labs, Hudson, NH, Plasmaspec III instrument) was performed by Ted J. Huston, Department of Geological Sciences, University of Michigan, Ann Arbor; ICP of iNOS samples (Jarrell-Ash, Waltham, MA, Atomscan 25 instrument) was performed by Saman Shafaie (Analytical Services Laboratory, Northwestern University, Evanston, IL). Graphite furnace atomic absorption spectroscopy analysis was performed on a Perkin–Elmer 2380 atomic absorption spectrophotometer controlled by a Perkin–Elmer HGA-400 programmer.

iNOS Activity Assays. Assays measuring citrulline production (300 μl total volume) contained variable amounts of nonheme iron or other transition metals and iNOS, 1 mM L-[^{14}C]arginine (1.5 mCi/mmol), 100 μM H_4B, 1 mM DTT, and 5 mM NADPH in Hepes buffer, pH 7.4. Identical conditions with unlabeled L-arginine were applied to iNOS used in turnover spectral experiments with the exception that the total volume was 600 μl. iNOS assays were run either at 25°C for 2.5 min or 0°C (on ice) for the indicated time course. All iNOS assay were performed in duplicate and the average values were plotted. No variation in duplicates was greater than 5% and most were ≈3%.

Electronic Absorption Spectroscopy. Spectra were recorded on a Varian Cary 3E spectrophotometer at a constant temperature of either 10°C or 25°C maintained by a Neslab circulating water bath.

RESULTS

Nonheme Metal Content. Metal analysis of nNOS and iNOS after purification showed that both proteins were capable of binding transition metals (Table 1). nNOS was isolated with nearly an equivalent of copper per 160-kDa subunit. However, after incubation with Fe^{2+} in the presence of L-arginine, H_4B and DTT as described in the methods, the enzyme was found to incorporate an equivalent of iron that apparently had replaced the previously bound copper (Table 1). iNOS, on the other hand, was isolated with 0.36 equivalents of Zn^{2+} per 130-kDa subunit. This isoform could also be reconstituted with a stoichiometric equivalent of iron under the same conditions as those for nNOS. Based on amino acid sequence similarity to the nonheme iron binding site of lysyl hydroxylase, H652 of nNOS was identified as a potential nonheme iron ligand. ICP analysis of the H652A mutant showed that this protein did not contain any copper or nonheme iron above the background levels of the buffer (<160 nM for copper, <220 nM for iron, the limits of ICP detection).

Influence of Nonheme Iron and Copper on Enzymatic Activity. The specific activity of nNOS with an equivalent of bound copper was 548 ± 10 nmol·min^{-1}·mg^{-1}. After exposure to DTT (as described below) nNOS contained no detectable copper and the specific activity of this preparation was 591 ± 19 nmol·min^{-1}·mg^{-1}. Because transition metal contamination could complicate the results, adventitious metals were removed by chelation as described in the methods. When nNOS was assayed in this metal-depleted buffer, no activity was detected in the presence of 30 μM $CuCl_2$. A time course of the Cu-inhibited reaction (20 μM $CuCl_2$) in metal-depleted buffer is shown in Fig. 1 (*Upper*, ○). These assays were carried out at 37°C, contained 30 nM nNOS, and were done in either duplicate or triplicate.

The effect of iron on NOS activity was examined next. One of the standard NOS activity assays follows the formation of the amino acid end product L-citrulline by separation from the radiolabeled substrate L-arginine on cation exchange (16). The NOS concentration typically used in such assays is 30 nM, and reactions are usually carried out at 37°C. Under these conditions, no inhibition of nNOS by nonheme iron (supplied as $FeCl_2$) was observed at the concentrations examined, up to 80 μM; in fact, variable increases in specific activity (up to 920 nmol·min^{-1}·mg^{-1}) were measured. When the enzyme was assayed in metal depleted buffer, a nonlinear rate of citrulline formation was observed (Fig. 1 *Upper*, ▼). However, when 10 μM $FeCl_2$ was added to this reaction, the rate was linear throughout the time course (Fig. 1 *Upper*, ●). At longer time points, the rate with no additions began to approach the rate observed after the addition of iron. Even after metal chelation from the assay buffers and reagents, the total assay mixture still retained ≈100 nM residual nonheme iron. Because the nNOS assay concentration was ≈30 nM, it was possible that iron reconstitution was taking place during the course of the assay. This hypothesis was addressed by carrying out assays in the presence of increasing concentrations of enzyme. Experiments with both nNOS (Fig. 1 *Lower*) and iNOS (data not

Table 1. Nonheme metal content for various preparations of NOS

Isoform	Conditions	Nonheme metal	Stoichiometry
Neuronal	As isolated	Cu	0.89 ± 0.03 (n = 3)
	Reconstituted	Fe	0.98 ± 0.10 (n = 5)
Inducible	As isolated	Zn	0.36 ± 0.04 (n = 2)
	Reconstituted	Fe	1.07 ± 0.13 (n = 3)

Samples were prepared for metal analysis as described in *Materials and Methods*. Metal quantitation for the "as isolated" samples was performed by ICP, and metal quantitation for the reconstituted samples was performed by graphite furnace atomic absorption (GF-AA). Although nonheme iron was always present with both isoforms as isolated, the stoichiometry was not consistent from preparation to preparation: measured values (both ICP and GF-AA) ranged from ≈0.15 to ≈0.40 equivalents per subunit [total iron (heme and nonheme) was 1.15–1.40].

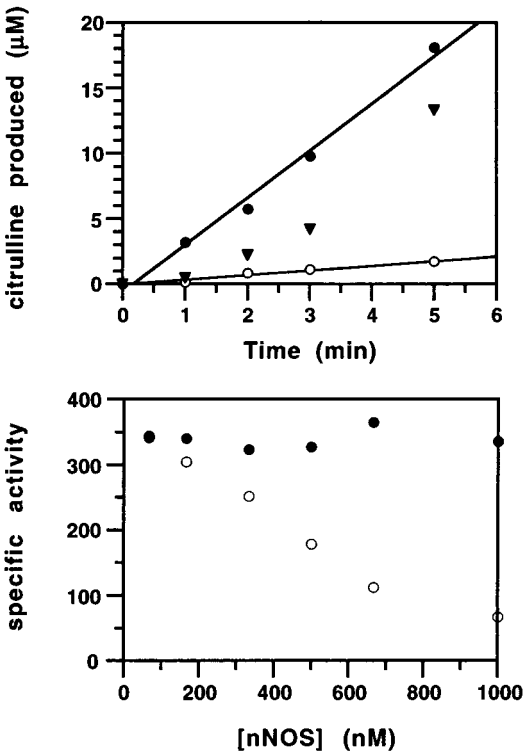

FIG. 1. nNOS catalysis in metal-depleted buffer. (*Upper*) Effect of transition metals on nNOS catalysis during typical assay conditions [≈30 nM nNOS, 37°C, 100 μM L-[^{14}C]arginine (1.5 mCi/mmol), 10 μM H_4B, 100 μM DTT, 1 mM $CaCl_2$, 100 nM calmodulin, and 500 μM NADPH, pH 7.4]; after chelation treatment this mixture retained ≈100 nM nonheme iron. The assay volume was 300 μl. ▼, nNOS activity in the absence of exogenous transition metals, showing an initial lag in citrulline formation that is not observed when the reaction is carried out in the presence of 10 μM $FeCl_2$ (●). ○, The inhibitory effect of 20 μM $CuCl_2$ added to the assays. Assays were done in triplicate and plotted as the mean. Absolute values varied less than 5%. (*Lower*) Effect of increasing nNOS concentration (67 nM to 1.0 μM) on the specific activity (nmol·min^{-1}·mg^{-1}), in the presence (●) and absence (○) of 20 μM added $FeCl_2$. The assays were carried out at 37°C for 2 min in the presence of 500 μM L-arginine. Assays were done in duplicate and plotted as the mean. Absolute values varied <5%.

shown) showed a progressive decrease in the specific activity on increasing enzyme concentration. In addition, an otherwise identical set of reactions performed in the presence of 20 μM added $FeCl_2$ showed that the specific activity could be maintained over the range of nNOS concentrations examined.

To further explore the effect of iron on the reaction the iNOS isoform was used. This isoform is not subject to substrate inhibition, and therefore could be assayed at high enzyme concentrations without the complicating feature of inhibition at saturating concentrations of L-arginine. iNOS was assayed at 25°C over a range of concentrations from 0.125 to 1.5 μM in the presence of saturating L-arginine (1 mM) and NADPH (5 mM). When these assays were not supplemented with nonheme iron (Fig. 2 *Upper*, ●), product formation was linear up to > 1 μM iNOS, consistent with a small population of iNOS retaining bound nonheme iron throughout the purification procedure. However, when 20 μM $FeCl_2$ was included in the assay mixture, the reaction ceased after 100 μM (≈30 nmol in 300 μl) L-citrulline had formed (Fig. 2 *Upper*, ○). Because NOS consumes at least 2 mol of oxygen per mol of citrulline formed, and the typical dissolved oxygen concentration is only ≈230 μM at 25°C, it is possible that the iron-supplemented reactions became depleted of this substrate. Experiments in which the concentration of oxygen was varied demonstrated that this was indeed the case (data not shown).

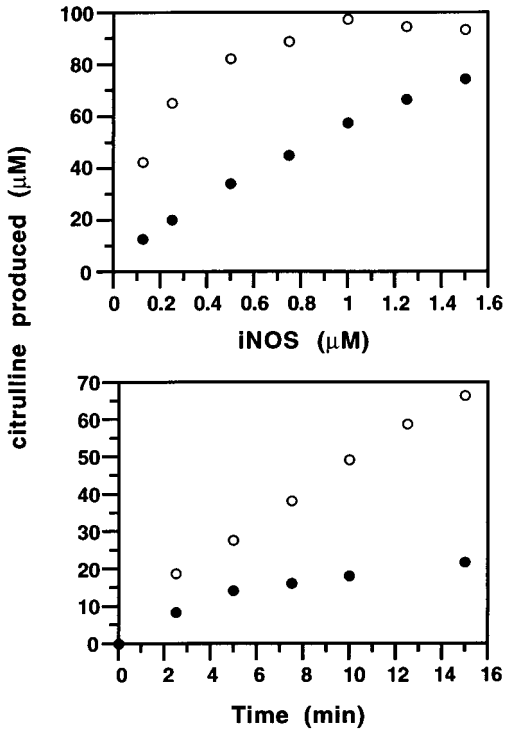

FIG. 2. Potentiation of iNOS activity by nonheme iron. The upper panel compares the amount of citrulline formed by various amounts of iNOS after 2.5 min in the presence (○) and absence (●) of 20 μM $FeCl_2$ at 25°C. Saturation of the effect in the presence of nonheme iron reflects the presumed depletion of oxygen. The lower panel is an activity time course of 500 nM iNOS in the presence (○) and absence (●) of 20 μM $FeCl_2$ when assayed at 0°C. This panel demonstrates that the addition of nonheme iron may have two stimulatory effects, one on the initial rate of product formation, and one on the steady-state rate.

When the reactions were carried out on ice (0°C), catalysis (and concomitant oxygen consumption) was slowed to a rate that allowed the observation of steady-state turnover of iNOS in the presence of $FeCl_2$ (Fig. 2 *Lower*). The iNOS rates of product formation in the presence and absence of 20 μM $FeCl_2$ at both 0°C and 25°C resulted in a 3-fold increase in activity at both temperatures; 22.3 ± 3.7 increased to 68.1 ± 4.2 nmol·min^{-1}·mg^{-1} at 0°C, and 365 ± 20 increased to 1112 ± 36 nmol·min^{-1}·mg^{-1} at 25°C, and all assays were carried out in either duplicate or triplicate. If the initial apparent burst phase is neglected and the linear steady-state rates observed at 0°C are directly compared, the rate increase is slightly over 5-fold (Fig. 2 *Lower*). This implies ≈30% productive occupancy of the iNOS nonheme iron site (in the absence of exogenous $FeCl_2$), which is presumably a combination of the population of iNOS that retains iron throughout the purification procedure and the population of iNOS that is reconstituted during the assay by residual iron in the assay components.

The effect of increasing concentrations of iron was examined under conditions where no substrate, including oxygen, would be limiting. As shown in Fig. 3 (*Upper*), the effect of iron was saturable with the maximal stimulation achieved with the addition of ≈12 μM $FeCl_2$. In addition, when the baseline activity was subtracted from the linear portion of the data, it was observed that 3 mol of citrulline was produced per mol of $FeCl_2$ added, indicating that the activation effects observed by the addition of iron result from multiple turnovers, and therefore, are not stoichiometric in nature (Fig. 3 *Lower*).

Effect of Other Transition Metals on Activity. Because Fe^{2+} stimulated the reaction, the specificity of this effect was studied further. iNOS was assayed in the presence of Cu^{2+}, Ni^{2+}, Mn^{2+}, Zn^{2+}, and Co^{2+} (added as the Cl^- salts) and, as shown in Fig. 4,

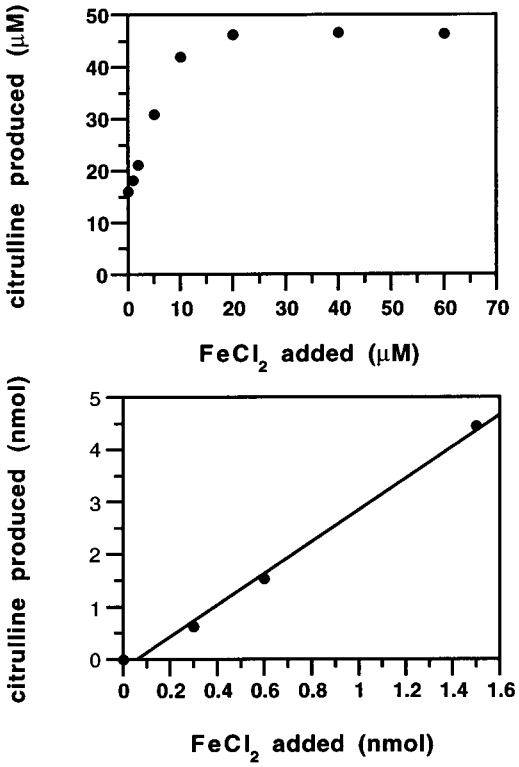

FIG. 3. Saturation and catalytic nature of the activation of iNOS catalysis by nonheme iron. (*Upper*) The saturability of the stimulatory effect of nonheme iron on iNOS catalysis; the iNOS concentration was fixed at 125 nM, and the reactions progressed for 2.5 min at 25°C. (*Lower*) The catalytic nature of the added nonheme iron, as 3 nmol of citrulline are formed per nmol of $FeCl_2$ added. Points were replotted from the linear portion of *Upper* with subtraction of the baseline activity in the absence of added iron. This baseline activity is attributed to the additive effects of residual nonheme iron in the assay mixture and a small population of iNOS purifying with nonheme iron bound.

all other metals tested inhibited the reaction with the exception of Mn^{2+}, which was without effect (serving also as a control for ionic strength).

Spectral Characterization of Metal Additions. As isolated, the NOS heme is predominantly high-spin with a Soret maximum at ≈400 nm. Fig. 5 (*Upper*) shows a typical spectrum of this type for iNOS as isolated and further shows that the addition of 30 μM $FeCl_2$ had minimal effects on the spectrum. Finally, when the iron-treated enzyme is reduced by NADPH in the presence of CO, the expected P450 spectrum is generated; hence, the added iron does not inhibit electron transfer from the flavins to the heme. Fig. 5 (*Lower*) shows the corresponding result when $CuCl_2$ is added. The addition of Cu^{2+} leads to greater change in the initial spectrum than that observed after the addition of Fe^{2+}, and the subtraction of these two spectra shows what appears to be a typical ligand to metal charge-transfer band (data not shown). The addition of Cu^{2+} clearly inhibits NADPH-supported heme reduction and, in the presence of CO, no P450 spectrum is generated. The spectrum shows that flavin reduction occurs, but that heme reduction does not; however, the subsequent addition of dithionite resulted in the formation of the expected P450 spectrum, providing evidence that the addition of Cu^{2+} did not greatly disrupt the heme environment.

Spectral experiments were also carried out with the H652A mutant and the results were similar to those obtained with the Cu-treated wild-type enzyme. As shown in Fig. 6 (*Upper*), the heme in this mutant as isolated is low-spin. NADPH treatment in the presence of CO reduces the flavins; however, like the Cu-treated wild-type enzyme, subsequent electron transfer to the heme is apparently blocked as the formation of a ferrous-CO

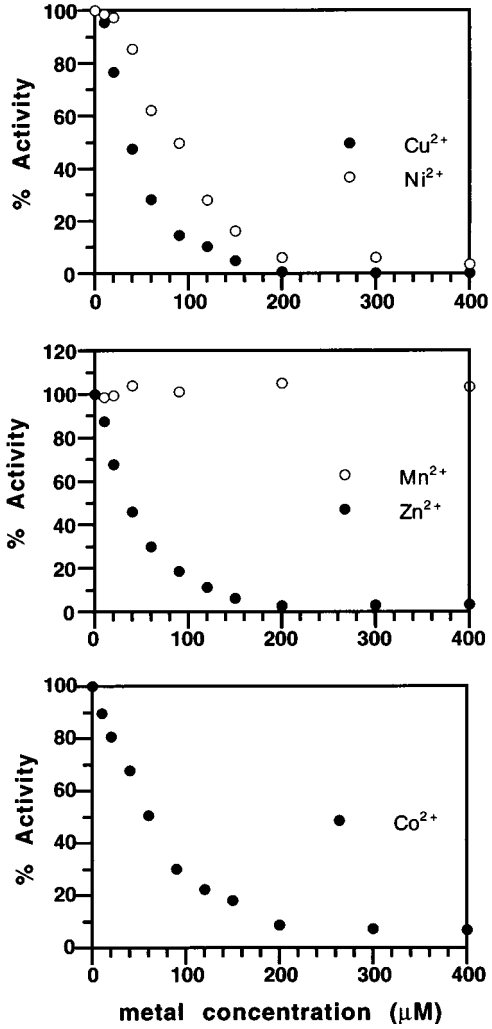

FIG. 4. Effect of other transition metals on iNOS activity. The indicated metals were added as their chloride salts to the given concentration; the iNOS concentration was 125 nM. All of the assays were carried out at 37°C for 3 min, and the final concentrations of the other components were as follows: 250 μM L-[^{14}C]arginine (1.5 mCi/mmol), 25 μM H_4B, 250 μM DTT, and 1 mM NADPH. All reactions were carried out in 50 mM Hepes buffer, pH 7.4, that had been pretreated with Chelex-100, and the reactions were initiated with NADPH.

complex was not observed. The integrity of the heme environment is apparently preserved in spite of the mutation because dithionite reduction in the presence of CO again led to the expected P450 Soret maximum (Fig. 6 *Upper*).

Nitrosyl Complex Formation. Product-mediated inhibition of NOS catalysis has been proposed to occur upon the binding of NO to the ferrous heme resulting in a ferrous nitrosyl complex (λ_{max} at 436 nm) (17); therefore, the possibility was addressed that the augmented citrulline production observed in the presence of added iron was merely an indirect effect of NO scavenging. Electronic absorption spectra of iNOS under conditions identical to the activity studies presented in Fig. 2 demonstrate that in the absence of exogenous iron, the NOS heme during turnover was a mixture of the NO bound species and the uncomplexed, high spin ferrous species (data not shown). However, in the presence of 20 μM $FeCl_2$, but under otherwise identical conditions, the heme undergoes conversion primarily to the nitrosyl complex (data not shown). When the same set of experiments was carried out at 10°C, identical results were obtained (within 10 sec of initiation of turnover) although product formation was linear for several minutes. This is consistent with the hypothesis that the stimulation of catalysis observed in the presence of nonheme iron

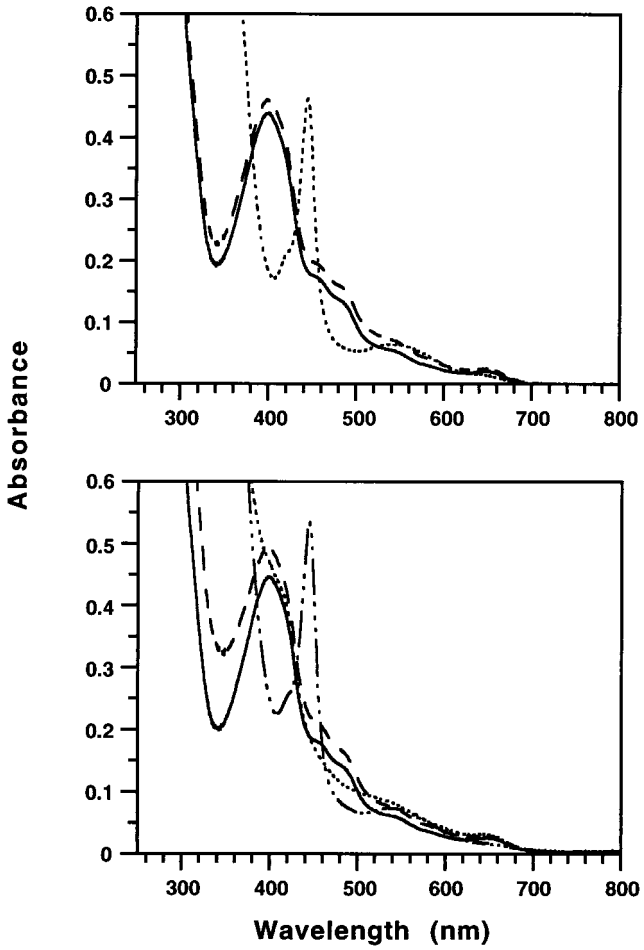

FIG. 5. Electronic absorption spectra of iNOS in the presence of iron and copper. All spectra were recorded at 10°C and the concentration of iNOS was ≈5 μM. (*Upper*) Effect of the addition of iron: (—) iNOS as isolated; (— —) iNOS after the addition of 30 μM $FeCl_2$ (- - -) iNOS after the subsequent addition of CO and NADPH (200 μM). (*Lower*) Effect of the addition of copper: (—) iNOS as isolated; (— —) iNOS after the addition of $CuCl_2$ to 100 μM; (- - -) iNOS after the subsequent addition of CO and NADPH (200 μM); and (— - - - —) iNOS mixture (iNOS, Cu, CO, NADPH) after the addition of dithionite.

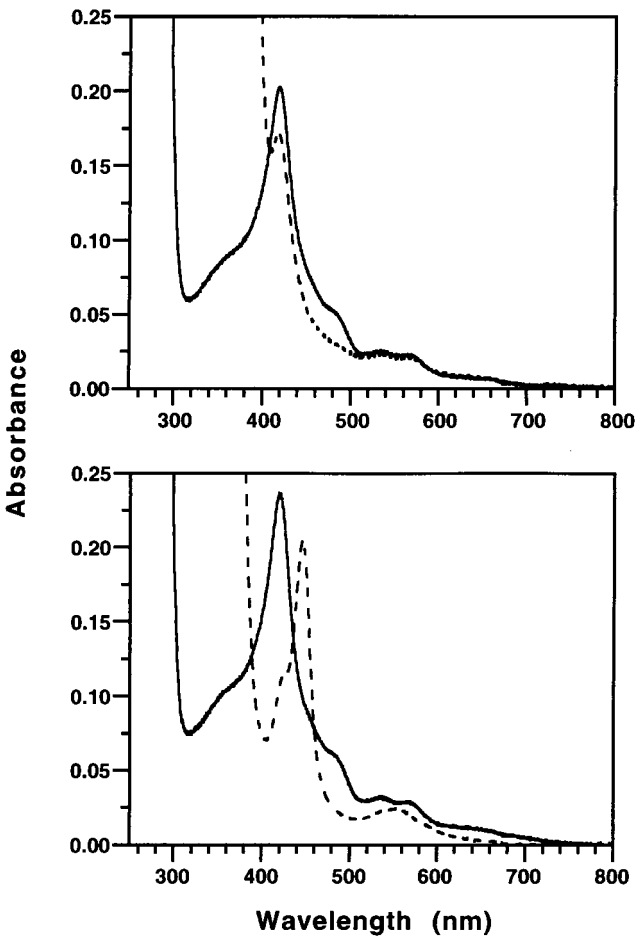

FIG. 6. Electronic absorption spectra of the H652A mutant of nNOS. All spectra were recorded at 10°C and the concentration of nNOS H652A was ≈3 μM. (*Upper*) The H652A mutation results in an inhibition of NADPH-dependent heme reduction: (– – –) is H652A as isolated and (—) is H652A after the equilibration with CO and subsequent addition of NADPH (200 μM). (*Lower*) H652A as isolated (—) and H652A after the equilibration with CO and subsequent addition of dithionite (– – –).

is the result of enhanced product formation and not the relief of a product mediated inhibition mechanism.

DISCUSSION

The results presented here demonstrate that NOS can bind divalent transition metals; however, only the addition of nonheme iron leads to an increase in catalytic activity. The fact that both nNOS (Cu) and iNOS (Zn) were initially isolated with bound transition metals that inhibit the reaction has precedent. For example, phenylalanine hydroxylase (PAH, a H_4B-dependent enzyme) isolated from *Chromobacterium violaceum* with a bound copper atom has been studied in detail (18–20). The specific activity of the *C. violaceum* PAH containing a full complement of copper was determined to be essentially identical to those preparations containing no detectable copper, and when excess copper was included in the PAH assays, it strongly inhibited catalysis (19). Our results with NOS are strikingly similar to those with the *C. violaceum* PAH. For *C. violaceum* PAH, it was determined that the protein-bound copper atom was extracted during the assay by DTT (19). The standard NOS assay also includes DTT, and when copper-saturated nNOS was exposed to the assay conditions, the removal of the bound copper atom was likewise observed. However, as shown above, nonheme iron can bind to NOS under similar conditions and both nNOS and iNOS can be reconstituted to 1 equivalent of nonheme iron per subunit when treated as described in Table 1. Inhibition of nonheme iron-dependent enzymes by other transition metals has also been observed. Examples include: isopenicillin-N synthase (Cu, Co), PAH (Cu, Zn), taurine dioxygenase (Cu, Zn), and clavaminate synthase (Zn, Co) (19, 21–23). In addition, zinc has previously been reported to bind to nNOS and inhibit catalytic activity (24).

All of the results presented here are consistent with the involvement of nonheme iron in NOS catalysis. The direct examination of this was hampered by the residual iron content of treated buffers, the residual nonheme iron bound to the enzyme, and the difficulties associated with assaying NOS at high concentrations in an effort to minimize the effect of residual iron. The same types of difficulties have been faced by others attempting to investigate the role of nonheme iron-dependent hydroxylations. Nonetheless, we have been able to observe stimulation of activity with added iron and, importantly, the effect is saturable. Further, we have provided evidence that this potentiation by iron is not due to solution scavenging of NO. If the added iron simply catalyzed the decomposition of NO in solution, it should have prevented the formation of a potentially inhibitory iron-nitrosyl complex. In contrast, we found that in the presence of added iron a higher percentage of this nitrosyl complex was formed.

The initial proposal for a chemical mechanism of NOS divided the reaction into two steps (25, 26). The first step was proposed to be the hydroxylation of L-arginine to NHA and the second involved the conversion of NHA to citrulline and NO. Subse-

quently it was shown that NHA is indeed formed during the course of the NOS reaction (6, 7), and biochemical studies have since supported a direct role for the P450 heme cofactor in that step of the reaction (8, 9). In addition, those studies also suggested that a cofactor other than the heme may be involved in the first step of reaction, and to date, no direct evidence links the P450 heme to the first step. Our results with transition metals and the well-established precedent for iron-H_4B coupled hydroxylations suggest the possibility of a direct chemical role for the reduced pterin in the reaction.

Alignment of the known NOS sequences and comparison to enzymes that catalyze iron-dependent hydroxylations such as lysyl hydroxylase led us to a tentative site that could provide the ligands required for metal binding. Lysyl hydroxylase contains an amino acid sequence [HHDAST$(X)_{15}$GGC] that donates two ligands, the first H and the D, to the active site nonheme iron (27). The homologous region of NOS, which is completely conserved among all the known sequences, is very similar to that of lysyl hydroxylase (DHH followed by a combination of S, A, and T; the D and the second H (H652 in nNOS) could serve as iron ligands). Consistent with this idea, the H652A point mutation generated an nNOS that was devoid of copper after purification (0.03 ± 0.01 copper/subunit; $n = 2$) and had no detectable catalytic activity, even in the presence of 80 μM $FeCl_2$. However, as shown in Fig. 6, H652A was still able to bind the heme cofactor and yield the signature electronic absorbance spectrum (λ_{max} at 444 nm) when reduced by dithionite in the presence of carbon monoxide. As a caveat, H652A was exclusively monomeric and structural effects of this point mutation beyond the heme binding site are not known.

The recently reported NOS heme domain structure crystallized with H_4B and L-arginine shows a spatial relationship between the pterin, the heme and L-arginine that does not appear, because of the distance between H_4B and arginine, to support the direct involvement of H_4B in the reaction (28). In this structure, the heme plane is perpendicular to the plane of the pterin with a hydrogen bond between the propionate residue of heme ring A and the pterin N3, whereas the guanidine moiety of L-arginine appears to be anchored in close proximity to the heme iron. This structure, however, did not show any bound nonheme metal. This is understandable given that the protein was a His-tag fusion protein that had been purified by a Ni resin, and hence exposed to a high concentration of imidazole. In addition, the high salt used in the crystallization could also result in the removal of any bound metal ions. If a pterin/metal complex is directly involved in the hydroxylation of L-arginine, the metal must bind above the C-4a position of the pterin ring, because the presumed hydroperoxide intermediate would form at this position after reaction with oxygen. In the reported structure, the edge of the pterin ring containing the C-4a position is exposed. Furthermore, it appears that a simple rotation around the Cα—Cβ bond of L-arginine would position the guanidine moiety over the pterin ring in an orientation in which hydroxylation could take place. It is also possible that in the crystal structure L-arginine has been frozen into one of two possible conformations due to the high salt used in the crystallization. In addition, the structure was solved with only 50% occupancy of bound substrate.

As described above, the H652A mutant has no nonheme iron or copper and is devoid of catalytic activity. The H652 (H431 in iNOS) residue appears to be close to the dimer interface, but lying above the heme plane. It is conceivable that upon iron binding to this residue and the proposed aspartate (from the comparison to lysyl hydroxylase D650 (D429 in iNOS) the iron could move into position above the edge of the pterin ring. There is also a conserved histidine (H692; H471 in iNOS) that lies above the heme plane and in proximity to the C-4a pterin edge. These three ligands in combination could serve to coordinate the nonheme iron and position the metal in proximity to the oxygen reactive site of the pterin.

The data presented here clearly show that NOS binds transition metals and, when included in the assays, only iron increases the rate of the reaction whereas the others tested either inhibited the reaction (Ni, Cu, Zn, and Co) or were without effect (Mn). Although the precise function of nonheme iron in NOS catalysis remains open for discussion, in conjunction with the literature precedent for iron/H_4B mediated hydroxylations of aromatic amino acids, the results suggest that the nonheme iron of NOS could function in concert with H_4B to form NHA from L-arginine. Further, the inability of hydrogen peroxide to substitute for NADPH and molecular oxygen in the conversion of L-arginine to NHA implies that the NOS heme may not be involved in this process that is minimally consistent with the participation of an alternate cofactor, perhaps an iron/H_4B complex (8, 9). Of course, additional or alternative roles of nonheme iron in NOS catalysis cannot be eliminated and are being explored.

We thank Prof. Perry A. Frey (University of Wisconsin, Madison) and Yunde Zhao for helpful discussions, Michelle M. Spiering for the iNOS expression system, Dr. Regina Stevens-Truss for advice and assistance, Drs. Kimberly A. White and Melissa J. Clague for their initial attempts to characterize nonheme metals in NOS, and members of the Marletta laboratory for their critical review of the manuscript. This work was supported by the National Institutes of Health. M.A.M. is an investigator of the Howard Hughes Medical Institute.

1. Jaffrey, S. R. & Snyder, S. H. (1996) *Science* **274,** 774–776.
2. Marletta, M. A. (1994) *Cell* **78,** 927–930.
3. White, K. A. & Marletta, M. A. (1992) *Biochemistry* **31,** 6627–6631.
4. Richards, M. K. & Marletta, M. A. (1994) *Biochemistry* **33,** 14723–14732.
5. Crane, B. R., Arvai, A. S., Gachhui, R., Wu, C., Ghosh, D. K., Getzoff, E. D., Stuehr, D. J. & Tainer, J. A. (1997) *Science* **278,** 425–431.
6. Stuehr, D. J., Kwon, N. S., Nathan, C. F., Griffith, O. W., Feldman, P. L. & Wiseman, J. (1991) *J. Biol. Chem.* **266,** 6259–6263.
7. Pufahl, R. A., Nanjappan, P. G., Woodard, R. W. & Marletta, M. A. (1992) *Biochemistry* **31,** 6822–6828.
8. Pufahl, R. A., Wishnok, J. S. & Marletta, M. A. (1995) *Biochemistry* **34,** 1930–1941.
9. Clague, M. J., Wishnok, J. S. & Marletta, M. A. (1997) *Biochemistry* **36,** 14465–14473.
10. Giovanelli, J., Campos, K. L. & Kaufman, S. (1991) *Proc. Natl. Acad. Sci. USA* **88,** 7091–7095.
11. Griscavage, J. M., Fukuto, J. M., Komori, Y. & Ignarro, L. J. (1994) *J. Biol. Chem.* **269,** 21644–21649.
12. Hevel, J. M. & Marletta, M. A. (1992) *Biochemistry* **31,** 7160–7165.
13. Perry, J. M., Moon, N., Zhao, Y., Dunham, W. R. & Marletta, M. A. (1998) *Chem. Biol.* **5,** 355–364.
14. Fossetta, J. D., Niu, X. D., Lunn, C. A., Zavodny, P. J., Narula, S. K. & Lundell, D. (1996) *FEBS Lett.* **379,** 135–138.
15. Bradford, M. M. (1976) *Anal. Biochem.* **72,** 248–254.
16. Hevel, J. M. & Marletta, M. A. (1994) *Methods Enzymol.* **233,** 250–258.
17. Hurshman, A. R. & Marletta, M. A. (1995) *Biochemistry* **34,** 5627–5634.
18. Pember, S. O., Villafranca, J. J. & Benkovic, S. J. (1986) *Biochemistry* **25,** 6611–6619.
19. Carr, R. T. & Benkovic, S. J. (1993) *Biochemistry* **32,** 14132–14138.
20. Chen, D. & Frey, P. A. (1998) *J. Biol. Chem.* **273,** in press.
21. Ming, L.-J., Jr., Que, L., Kriauciunas, A., Frolik, C. A. & Chen, V. J. (1990) *Inorg. Chem.* **29,** 1111–1112.
22. Eichhorn, E., Ploeg, J. R. v. d., Kertesz, M. A. & Leisinger, T. (1997) *J. Biol. Chem.* **272,** 23031–23036.
23. Busby, R. W., Chang, M. D., Busby, R. C., Wimp, J. & Townsend, C. A. (1995) *J. Biol. Chem.* **270,** 4262–4269.
24. Persechini, A., McMillan, K. & Masters, B. S. S. (1995) *Biochemistry* **34,** 15091–15095.
25. Marletta, M. A., Yoon, P. S., Iyengar, R., Leaf, C. D. & Wishnok, J. S. (1988) *Biochemistry* **27,** 8706–8711.
26. Marletta, M. A. (1993) *J. Biol. Chem.* **268,** 12231–12234.
27. Pirskanen, A., Kaimio, A.-M., Myllylä, R. & Kivirikko, K. I. (1996) *J. Biol. Chem.* **271,** 9398–9402.
28. Crane, B. R., Arvai, A. S., Ghosh, D. K., Wu, C., Getzoff, E. D., Stuehr, D. J. & Tainer, J. A. (1998) *Science* **279,** 2121–2126.